

# C–O and C–S Bonds: Stability, Bond Dissociation Energies, and Resonance Stabilization

Christopher M. Hadad,<sup>\*†</sup> Paul R. Rablen,<sup>\*‡</sup> and Kenneth B. Wiberg<sup>\*§</sup>

Department of Chemistry, The Ohio State University, Columbus, Ohio 43210, Department of Chemistry, Swarthmore College, Swarthmore, Pennsylvania 19081, and Department of Chemistry, Yale University, New Haven, Connecticut 06511

Received December 2, 1997

The structures and energies of the compounds X–C(=O)OH, X–C(=S)OH, X–C(=O)SH, and X–C(=S)SH, where X = CH<sub>3</sub>, NH<sub>2</sub>, OH, and F, were obtained at the MP2/6-31+G(2d) theoretical level, and energies were calculated at the MP3/6-311++G(2d,p), CBS-4, and G2 theoretical levels. These data show that X–C(=O)SH is preferred over X–C(=S)OH by 5 kcal/mol with X = CH<sub>3</sub>, and the preference increases to 12 kcal/mol with X = F. The C–O(H) bond dissociation energies were greater than the C–S(H) energies by approximately 30 kcal/mol and were only weakly affected by the nature of X attached to the carbonyl carbon. Calculated bond dissociation energies reveal that a C=O bond is significantly stronger than a C=S bond (by about 40 kcal/mol). The calculated atomic charges and bond orders demonstrated that a double bond to oxygen had a much larger effect on the attached carbon than did a single bond to oxygen. The C=O covalent bond orders were about 1.2, in accord with their considerable ionic character, while the C=S covalent bond orders were close to 2.0. Differences between the MP2/6-31+G(d) charge density for the ground state and the bond rotation transition state were used to investigate the nature of the electronic reorganization that occurs during bond rotation. This approach revealed that intramolecular charge transfer was greater for C–N bond rotation than for C–O bond rotation and greater for C–O rotation than for C–S rotation. Furthermore, polarization was greater for C=S than for C=O with all rotating groups by almost a factor of 2, in accord with the greater amount of charge transfer known to accompany bond rotation in thioamides as compared to amides. In all cases, the ground state exhibited charge transfer in the  $\pi$  system to the terminal carbonyl oxygen or thiocarbonyl sulfur atom that was partially counteracted by charge transfer in the  $\sigma$  system in the opposite direction.

## 1. Introduction

Thioesters figure prominently in biochemical pathways, and carbon–oxygen and carbon–sulfur bonds are ubiquitous in nature.<sup>1</sup> All four combinations of the form C(=X)–Y are known experimentally in biochemical contexts, where X and Y are sulfur and/or oxygen. Carboxylic acids are so common that they require no further comment. Thiol esters (the C(=O)–S fragment) are known as intermediates in the cleavage of peptides by cysteine proteases, which rely on the reactivity of sulfur for their activity. Thionoesters (the C(=S)–O fragment) can also be used as substrates for some cysteine proteases, such as papain.<sup>2</sup> The product is a dithioester (the C(=S)–S fragment), and substitution of thionoesters for the natural substrates in this manner has been used to shed light on the catalytic mechanism.<sup>2</sup> However, despite the existence of all four substitution patterns, carbon–sulfur double bonds are noticeably less prevalent than carbon–oxygen double bonds. We were interested in exploring the reasons for this apparent bias against the occurrence of C=S in natural systems.

We also wished to compare the structures and properties of simple compounds containing C=S bonds to those

containing C=O bonds, since the latter class of compounds has been the subject of a previous investigation. Our study of carbonyl bonds revealed that both the electronegativity and  $\pi$ -donating ability of an attached substituent led to stabilization of the carbonyl group.<sup>3</sup> Stabilization by electronegative elements such as fluorine resulted from cooperative electrostatic stabilization driven by the strongly polarized nature of the C=O bond, while the stabilization by  $\pi$  donors could be understood on the basis of a conventional HOMO–LUMO interaction or a modified resonance picture. As part of our ongoing investigation of substituent effects on thermodynamic stability and charge density distribution within various structural motifs, we present here our study of substituent effects on C–O and C–S bonds in simple systems via *ab initio* molecular orbital theory.

Some previous experimental and computational studies of thiocarbonyl compounds have been reported. Schwarz, Carlsen, and co-workers have recently studied dimethyl carbonate and its thio analogues via mass spectrometric methods and have shown that thio–carbonyl bonds (C=S) are thermodynamically less stable than carbonyl (C=O) bonds,<sup>4</sup> in agreement with the findings presented here. Abboud and co-workers have compared the gas-phase basicities of carbonyl and thiocarbonyl compounds, and also the substituent effects on those gas-phase

<sup>†</sup> The Ohio State University.

<sup>‡</sup> Swarthmore College.

<sup>§</sup> Yale University.

(1) For example, see: Stryer, L. *Biochemistry*, 3rd edition; W. H. Freeman & Company: New York, 1988.

(2) Duncan, G. D.; Huber, C. P.; Welsh, W. J. *J. Am. Chem. Soc.* **1992**, *114*, 5784 and references therein.

(3) Wiberg, K. B.; Hadad, C. M.; Rablen, P. R.; Cioslowski, J. *J. Am. Chem. Soc.* **1992**, *114*, 8644.

(4) Egsgaard, H.; Suelzle, D.; Schwarz, H.; Carlsen, L. *Chem. Ber.* **1991**, *124*, 1265.

basicities, using both experimental and computational approaches.<sup>5</sup> They found that reactivity patterns in thiocarbonyl compounds were similar qualitatively to those in carbonyl compounds but were less pronounced in a quantitative sense. Thioamides in particular have attracted abundant computational interest in the past.<sup>6,7</sup> The barriers to rotation about the C–N bonds of thioamides are known to be larger than those for simple amides, contrary to the expectations derived from simple resonance theory, and have been the subject of previous study.<sup>8</sup> The calculations presented here provide some information about the nature of the transition states for C–N bond rotation in thioamides and related thiocarbonyl compounds.

## 2. Methods

All *ab initio* calculations were carried out using the Gaussian 92<sup>9</sup> and Gaussian 94<sup>10</sup> software packages. Standard basis sets were used but always with six Cartesian d functions (the 6D option).<sup>11</sup> Geometry optimization was carried out at both the Hartree–Fock (HF) and second-order Møller–Plesset (MP2) levels of theory, using both the 6-31G(d) and 6-31+G(2d) basis sets. Unrestricted HF theory was used for all open-shell systems. Analytical evaluation of the Hessian matrix for the HF geometries was used in order to determine the zero-point vibrational energy and to characterize the type of stationary point; all vibrational frequencies were multiplied by the recommended scaling factor of 0.8934.<sup>12</sup> All optimizations allowed for the correlation of all electrons, but single-point energy calculations with the 6-311++G(2d,p) basis set utilized the frozen-core approximation. For the radicals considered here, spin contamination was very small, if present at all, and the calculated  $\langle S^2 \rangle$  values were less than 0.79.

Calculations of the atomic contributions to the molecular properties were performed with the Atoms in Molecules Package (AIMPAC) and the PROAIM program from McMaster University.<sup>13</sup> Covalent bond orders were

calculated according to the method of Cioslowski and Mixon, with a modified version of BONDER.<sup>14</sup>

It is known that large basis sets and extensive correction for electron correlation are often required to obtain accurate estimates of bond dissociation energies (BDEs). The G-2 model developed by Pople et al.<sup>15</sup> has been shown to be remarkably effective in reproducing relative energies, but it is computationally too demanding for examining all of the structures in this study. An attractive alternative is the CBS-4 method of Petersson and Ochterski<sup>16</sup> which reproduces relative energies with an accuracy only slightly diminished with respect to the G-2 method. The CBS-4 procedure makes use of a very large basis set HF calculation, corrections for electron correlation at the MP4(SDQ) level, and a complete basis set extrapolation. It also includes the zero-point energies and a higher-level correction similar to that in G-2. We have used the CBS-4 procedure for the majority of BDE calculations presented here, along with MP2 and MP3 calculations, but we have also included a few selected G-2 BDEs for the purpose of comparison.

Difference-density maps for C–N, C–O, and C–S rotation were obtained at the MP2/6-31+G(d) level of theory and visualized using the CASGEN software package written at Yale University. The ground-state structures of NH<sub>2</sub>C(=O)OH, NH<sub>2</sub>C(=O)SH, NH<sub>2</sub>C(=S)OH, and NH<sub>2</sub>C(=S)SH were optimized under C<sub>s</sub> symmetry. In those cases where the true ground state lacks this symmetry, the energetic cost of introducing the symmetry constraint was only slight. Partially optimized structures were then obtained for the transition states for C–N, C–O, and C–S bond rotation. In each case, the rotating part of the molecule (–SH, –OH, or –NH<sub>2</sub>) was allowed complete freedom, while the remainder was held frozen at the exact ground-state geometry. The geometric constraint is required in order to facilitate proper subtraction of the charge-density distributions in the next stage.

Correlated (MP2) wave functions were obtained for the ground-state and constrained-transition-state geometries via the density=current option in Gaussian. For each case, the charge density for the ground state was subtracted from that for the constrained transition state in order to obtain the corresponding difference density. The difference density thus generated was then depicted graphically as a three-dimensional surface representing the 0.002 e/b<sup>3</sup> contour. The large differences in charge density occurring in the immediate vicinity of the rotating NH<sub>2</sub>, OH, or SH group were removed to avoid confusion in visualizing the changes, since only charge-density shifts in the “frozen” portion of the molecule are interpretable in a straightforward manner. In particular, only the differences in the vicinity of the carbonyl oxygen (=O) or thiocarbonyl sulfur (=S) and the *stationary* NH<sub>2</sub>, OH, or SH substituent are meaningful. The double-bonded carbon atom (C=) is sufficiently close to the rotating portion of the molecule that charge-density shifts in its immediate vicinity cannot be differentiated reliably from changes resulting only from the actual motion of the neighboring atoms.

(5) Abboud, J.-L. M.; Mó, O.; de Paz, J. L. G.; Yáñez, M.; Esseffar, M.; Bouab, W.; El-Mouhtadi, M.; Mokhlisse, R.; Ballesteros, E.; Herreros, M.; Homan, H.; Lopez-Mardodomingo, C.; Notario, R. *J. Am. Chem. Soc.* **1993**, *115*, 12468.

(6) (a) Lim, K. T.; Francl, M. M. *J. Phys. Chem.* **1987**, *91*, 2716. (b) Wiberg, K. B.; Breneman, C. M. *J. Am. Chem. Soc.* **1992**, *114*, 831. (c) Ou, M.-C.; Tsai, M.-S.; Chu, S.-Y. *J. Mol. Struct.* **1994**, *310*, 247.

(7) Wiberg, K. B.; Rablen, P. R. *J. Am. Chem. Soc.* **1995**, *117*, 2201. (8) (a) Sandström, J. *J. Phys. Chem.* **1967**, *71*, 2318. (b) Neuman, R. C., Jr.; Young, L. B. *J. Phys. Chem.* **1965**, *69*, 2570. (c) Loewenstein, A.; Melera, A.; Rigny, P.; Walter, W. *J. Phys. Chem.* **1964**, *68*, 1597.

(9) Frisch, M. J.; Trucks, G. W.; Head-Gordon, M.; Gill, P. M. W.; Wong, M. W.; Foresman, J. B.; Johnson, B. G.; Schlegel, H. B.; Robb, M. A.; Replogle, E. S.; Gomperts, R.; Andres, J. L.; Raghavachari, K.; Binkley, J. S.; Gonzalez, C.; Martin, R. L.; Fox, D. J.; Defrees, D. J.; Baker, J.; Stewart, J. J. P.; Pople, J. A. *GAUSSIAN 92*, Revision A; Gaussian Inc.: Pittsburgh, PA, 1992.

(10) Frisch, M. J.; Trucks, G. W.; Schlegel, H. B.; Gill, P. M. W.; Johnson, B. G.; Robb, M. A.; Cheeseman, J. R.; Keith, T.; Petersson, G. A.; Montgomery, J. A.; Raghavachari, K.; Al-Laham, M. A.; Zakrzewski, V. G.; Ortiz, J. V.; Foresman, J. B.; Cioslowski, J.; Stefanov, B. B.; Nanayakkara, A.; Challacombe, M.; Peng, C. Y.; Ayala, P. Y.; Chen, W.; Wong, M. W.; Andres, J. L.; Replogle, E. S.; Gomperts, R.; Martin, R. L.; Fox, D. J.; Binkley, J. S.; Defrees, D. J.; Baker, J.; Stewart, J. J. P.; Head-Gordon, M.; Gonzalez, C.; Pople, J. A. *Gaussian 94*, Revision D.3; Gaussian, Inc.: Pittsburgh, PA, 1994.

(11) Hehre, W. J.; Radom, L.; Schleyer, P. v. R.; Pople, J. A. *Ab Initio Molecular Orbital Theory*; Wiley-Interscience: New York, 1986.

(12) Pople, J. A.; Head-Gordon, M.; Fox, D. J.; Raghavachari, K.; Curtiss, L. A. *J. Chem. Phys.* **1989**, *90*, 5622.

(13) (a) Biegler-König, F. W.; Bader, R. F. W.; Tang, T.-H. *J. Comput. Chem.* **1982**, *3*, 317. (b) Bader, R. F. W.; Tang, T.-H.; Tal, Y.; Biegler-König, F. W. *J. Am. Chem. Soc.* **1982**, *104*, 946.

(14) Cioslowski, J.; Mixon, S. T. *J. Am. Chem. Soc.* **1991**, *113*, 4142.

(15) Curtiss, L. A.; Raghavachari, K.; Trucks, G. W.; Pople, J. A. *J. Chem. Phys.* **1991**, *94*, 7221.

(16) (a) Ochterski, J.; Petersson, G.; Wiberg, K. B. *J. Am. Chem. Soc.* **1995**, *117*, 11299. (b) Ochterski, J.; Petersson, G.; Montgomery, J. A., Jr. *J. Chem. Phys.* **1996**, *104*, 2598.

Quantitation of the charge-density redistributions depicted by the difference-density plots was accomplished through numerical integration. For the difference densities corresponding to changes in the level of *ab initio* theory (e.g., change in basis set or in the level of treatment of electron correlation), the total difference density was simply integrated over all space, but with the positive and negative components summed separately. For the difference densities showing the effects of bond rotation, a somewhat more involved procedure was used in which integration of any given lobe was accomplished by integrating out from the center of the lobe to a boundary defined by a given contour level. This procedure is carried out for a standard series of contour levels, and then an extrapolation is made to the limit of a zero contour. The methodology has been described in detail elsewhere.<sup>7</sup>

### 3. Molecular Geometries

To carry out our study of carbonyl and thiocarbonyl compounds, we needed a level of *ab initio* theory that would provide reliable and accurate molecular structures at a reasonable computational cost. With this requirement in mind, we explored the effect of basis set (6-31G(d) and 6-31+G(2d)) and correlation treatment (HF and MP2) on the optimized geometries of the compounds  $\text{XH}_n\text{C}(=\text{O})-\text{OH}$ ,  $\text{XH}_n\text{C}(=\text{O})-\text{SH}$ ,  $\text{XH}_n\text{C}(=\text{S})-\text{OH}$ , and  $\text{XH}_n\text{C}(=\text{S})-\text{SH}$  ( $\text{XH}_n = \text{CH}_3, \text{NH}_2, \text{OH}, \text{and F}$ ) (Table 1). Bond lengths were consistently underestimated by 0.02–0.04 Å at the HF level in comparison with the more reliable MP2 calculations. The basis set was found to have a lesser effect, but we nonetheless settled on MP2/6-31+G(2d) as the most appropriate level of calculation for geometry optimization. The MP2/6-31+G(2d) procedure is an augmented version of the MP2/6-31G(d) procedure, and the latter has been extensively tested, is known to reproduce structures in close agreement with experiment for a wide variety of molecules, and is used in Pople's highly reliable G-2 procedure. Full details of our examination of basis set and correlation dependence of molecular geometry are included in the Supporting Information.

Table A in the Supporting Information lists the species calculated as part of this study along with their ground-state point groups and their energies at several levels of theory. The ground-state structures were found in all cases either to be planar ( $C_s$  symmetry) or, if nonplanar ( $C_1$  point group), to have only a very small energetic cost associated with planarization. In those cases where *E* and *Z* isomers were possible, the *Z* isomer was consistently preferred, in exact analogy to well-documented cases of acetic and formic acid.<sup>17</sup> Transition states for rotation about the C–X bonds ( $X = \text{OH}, \text{SH}, \text{and NH}_2$ ) were also computed for the series of compounds  $\text{H}_2\text{NC}(=\text{X})\text{YH}$ , where  $X = \text{O or S}$  and  $Y = \text{O or S}$ . The transition states for C–N bond rotation conformed naturally to  $C_s$  symmetry. The nature of each stationary point was confirmed by analytical calculation of the vibrational frequencies, i.e., no imaginary frequencies for minima and one imaginary frequency for transition states.

**Table 1. Selected Geometrical Parameters for Carbonyl and Thiocarbonyl Derivatives<sup>a</sup>**

parameter	$\text{XH}_n$	MP2/6-31+G(2d)	$\Delta\text{MP2}^b$	$\Delta(\text{MP2} - \text{RHF})^c$
$\text{XH}_n\text{C}(=\text{O})-\text{OH}$ Planar ( $C_s$ )				
$r(\text{C}=\text{O})$	$\text{CH}_3$	1.2109	–0.0061	+0.0278
	$\text{NH}_2$	1.2145	–0.0057	+0.0246
	$\text{OH}$	1.2086	–0.0067	+0.0251
	$\text{F}$	1.1912	–0.0084	+0.0249
$r(\text{C}-\text{O})$	$\text{CH}_3$	1.3577	–0.0035	+0.0282
	$\text{NH}_2$	1.3624	–0.0044	+0.0320
	$\text{OH}$	1.3390	–0.0051	+0.0267
	$\text{F}$	1.3305	–0.0071	+0.0252
$r(\text{C}-\text{X})$	$\text{CH}_3$	1.4967	–0.0035	–0.0041
	$\text{NH}_2$	1.3523	–0.0035	+0.0101
	$\text{OH}$	1.3390	–0.0051	+0.0267
	$\text{F}$	1.3327	–0.0016	+0.0376
$\text{XH}_n\text{C}(=\text{O})-\text{SH}$ Planar ( $C_s$ )				
$r(\text{C}=\text{O})$	$\text{CH}_3$	1.2106	–0.0063	+0.0320
	$\text{NH}_2$	1.2142	–0.0048	+0.0284
	$\text{OH}$	1.2058	–0.0063	+0.0287
	$\text{F}$	1.1874	–0.0086	+0.0277
$r(\text{C}-\text{S})$	$\text{CH}_3$	1.7979	+0.0001	+0.0021
	$\text{NH}_2$	1.8023	–0.0050	+0.0069
	$\text{OH}$	1.7698	–0.0033	–0.0014
	$\text{F}$	1.7527	–0.0061	–0.0063
$r(\text{C}-\text{X})$	$\text{CH}_3$	1.5051	–0.0021	–0.0038
	$\text{NH}_2$	1.3565	–0.0036	+0.0111
	$\text{OH}$	1.3499	–0.0040	+0.0298
	$\text{F}$	1.3606	+0.0050	+0.0474
$\text{XH}_n\text{C}(=\text{S})-\text{OH}$ Planar ( $C_s$ )				
$r(\text{C}=\text{S})$	$\text{CH}_3$	1.6290	–0.0003	–0.0009
	$\text{NH}_2$	1.6458	–0.0022	–0.0165
	$\text{OH}$	1.6368	–0.0019	–0.0121
	$\text{F}$	1.6123	–0.0027	–0.0055
$r(\text{C}-\text{O})$	$\text{CH}_3$	1.3465	–0.0029	+0.0346
	$\text{NH}_2$	1.3508	–0.0038	+0.0362
	$\text{OH}$	1.3304	–0.0052	+0.0331
	$\text{F}$	1.3252	–0.0068	+0.0325
$r(\text{C}-\text{X})$	$\text{CH}_3$	1.4933	–0.0033	–0.0038
	$\text{NH}_2$	1.3406	–0.0026	+0.0196
	$\text{OH}$	1.3304	–0.0052	+0.0331
	$\text{F}$	1.3291	–0.0012	+0.0418
$\text{XH}_n\text{C}(=\text{S})-\text{SH}$ Planar ( $C_s$ )				
$r(\text{C}=\text{S})$	$\text{CH}_3$	1.6301	+0.0019	+0.0122
	$\text{NH}_2$	1.6420	+0.0003	–0.0094
	$\text{OH}$	1.6297	+0.0003	–0.0011
	$\text{F}$	1.6067	–0.0006	+0.0064
$r(\text{C}-\text{S})$	$\text{CH}_3$	1.7584	+0.0003	+0.0034
	$\text{NH}_2$	1.7779	–0.0009	+0.0091
	$\text{OH}$	1.7561	–0.0007	+0.0042
	$\text{F}$	1.7467	–0.0028	+0.0006
$r(\text{C}-\text{X})$	$\text{CH}_3$	1.5058	–0.0011	–0.0025
	$\text{NH}_2$	1.3490	–0.0015	+0.0228
	$\text{OH}$	1.3459	–0.0039	+0.0365
	$\text{F}$	1.3561	+0.0020	+0.0479

<sup>a</sup> Distances in angstroms and angles in degrees. <sup>b</sup>  $\Delta\text{MP2}$  is the difference between the 6-31+G(2d) and the 6-31G(d) geometries at the MP2 level. <sup>c</sup> Difference between the MP2 and the RHF geometries with the 6-31+G(2d) basis set.

### 4. Effect of Basis Set and Correlation on Charge Distribution

A recent study has shown that, as a consequence of underestimating electron–electron repulsion, the HF theory tends to concentrate too much charge density between nuclei sharing a covalent bond.<sup>18</sup> Inclusion of electron correlation moves some of the charge density between bonded atoms to the periphery of the molecule in order to decrease electron–electron repulsion and results in somewhat longer bond lengths. This tendency

(17) (a) Wang, X.; Houk, K. N. *J. Am. Chem. Soc.* **1988**, *110*, 1870. (b) Wiberg, K. B.; Laidig, K. E. *J. Am. Chem. Soc.* **1988**, *110*, 1872.

(18) Wiberg, K. B.; Hadad, C. M.; LePage, T. L.; Breneman, C. M.; Frisch, M. J. *J. Phys. Chem.* **1992**, *96*, 671.

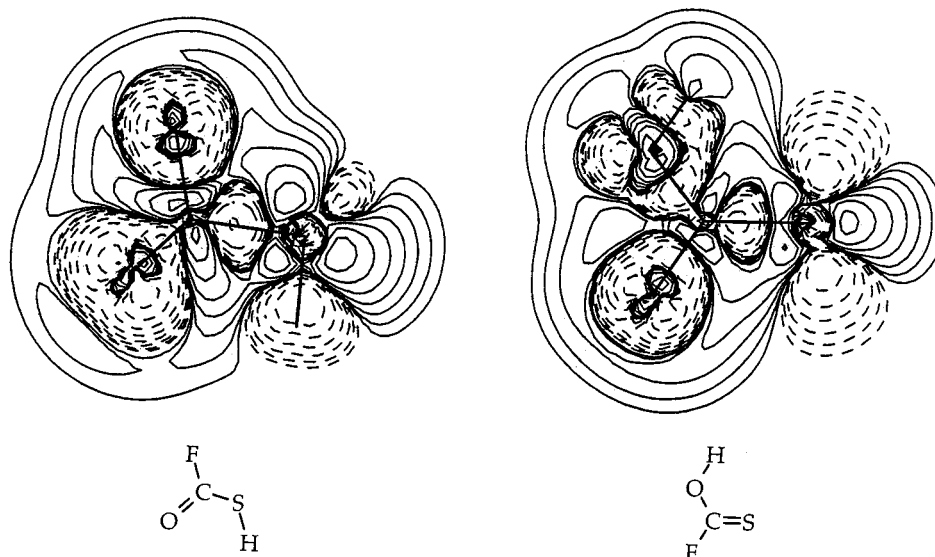


**Figure 1.** Effect of electron correlation: charge-density-difference plots for the molecular plane ( $\sigma$  system) of  $\text{FC}(=\text{O})\text{-SH}$  and  $\text{FC}(=\text{S})\text{-OH}$ . Left:  $\text{MP2}/6\text{-}31+\text{G}(2\text{d}) - \text{RHF}/6\text{-}31+\text{G}(2\text{d})$  for  $\text{FC}(=\text{O})\text{-SH}$ . Right:  $\text{MP2}/6\text{-}31+\text{G}(2\text{d}) - \text{RHF}/6\text{-}31+\text{G}(2\text{d})$  for  $\text{FC}(=\text{S})\text{-OH}$ . The outermost contour is  $0.0001 \text{ e}/b^3$  and increases by a factor of 2 for each successive contour.

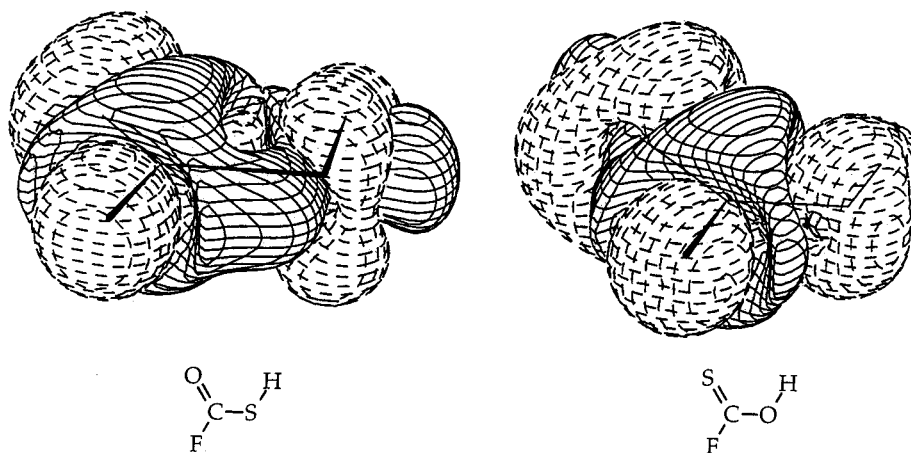


**Figure 2.** Effect of electron correlation: charge-density-difference plots for the total distribution of  $\text{FC}(=\text{O})\text{-SH}$  and  $\text{FC}(=\text{S})\text{-OH}$ . Left:  $\text{MP2}/6\text{-}31+\text{G}(2\text{d}) - \text{RHF}/6\text{-}31+\text{G}(2\text{d})$  for  $\text{FC}(=\text{O})\text{-SH}$ . Right:  $\text{MP2}/6\text{-}31+\text{G}(2\text{d}) - \text{RHF}/6\text{-}31+\text{G}(2\text{d})$  for  $\text{FC}(=\text{S})\text{-OH}$ . The outermost contour is  $0.0001 \text{ e}/b^3$ .

decreases or even reverses, however, for highly polar and ionic bonds, where electron correlation can actually lead to shorter bonds.

We have explored this effect by examining the changes in the charge density that occur upon the inclusion of electron correlation. Wave functions were calculated for  $\text{FC}(=\text{O})\text{-SH}$  and  $\text{FC}(=\text{S})\text{-OH}$  at the  $\text{RHF}/6\text{-}31\text{G}(\text{d})$ ,  $\text{RHF}/6\text{-}31+\text{G}(2\text{d})$ ,  $\text{MP2}/6\text{-}31\text{G}(\text{d})$ , and  $\text{MP2}/6\text{-}31+\text{G}(2\text{d})$  levels of theory using the  $\text{MP2}/6\text{-}31\text{G}(\text{d})$  optimized geometries. Three-dimensional cubic grids of charge-density values, 20 au and 81 grid points to a side, were then computed for each wave function. The HF cube was subtracted from the MP2 cube at each of the two basis sets to generate the difference densities shown in Figures 1 and 2, which then illustrate the charge-density redistribution associated with electron correlation. Figure 1 shows charge density in the molecular plane only ( $\sigma$  system), while Figure 2 shows the total three-dimensional charge distribution. For both figures, solid lines correspond to positive values for the density difference (i.e., more electron density with MP2 than with HF), and dashed lines correspond to negative values.

Figure 1 illustrates the changes in just the  $\sigma$  system, representing the difference density in the molecular plane as a conventional contour plot. As expected, electron correlation at the MP2 level causes charge density to accumulate in the diffuse regions of the molecules at the expense of the nuclei and the bonding regions, thereby causing the bond elongation. There is also a noticeable difference in how the various types of atoms are affected by electron correlation. The use of MP2 depletes charge density in the immediate vicinity of both fluorine and oxygen nuclei relative to HF and leads to a large accumulation on the periphery of the molecule. Sulfur, on the other hand, seems to be less affected. Thus, the extent of charge redistribution appears to be greatest for the most electronegative elements, which have a region of concentrated charge density near the nucleus that can benefit from a reduction in electron repulsion.

Figure 2 shows that the  $\pi$  system is affected as well. The "chicken-wire" surfaces in Figure 2 represent the isodensity contours in three dimensions where the difference density equals  $\pm 0.002 \text{ e}/b^3$ . It is readily apparent that MP2 correction increases the charge density between

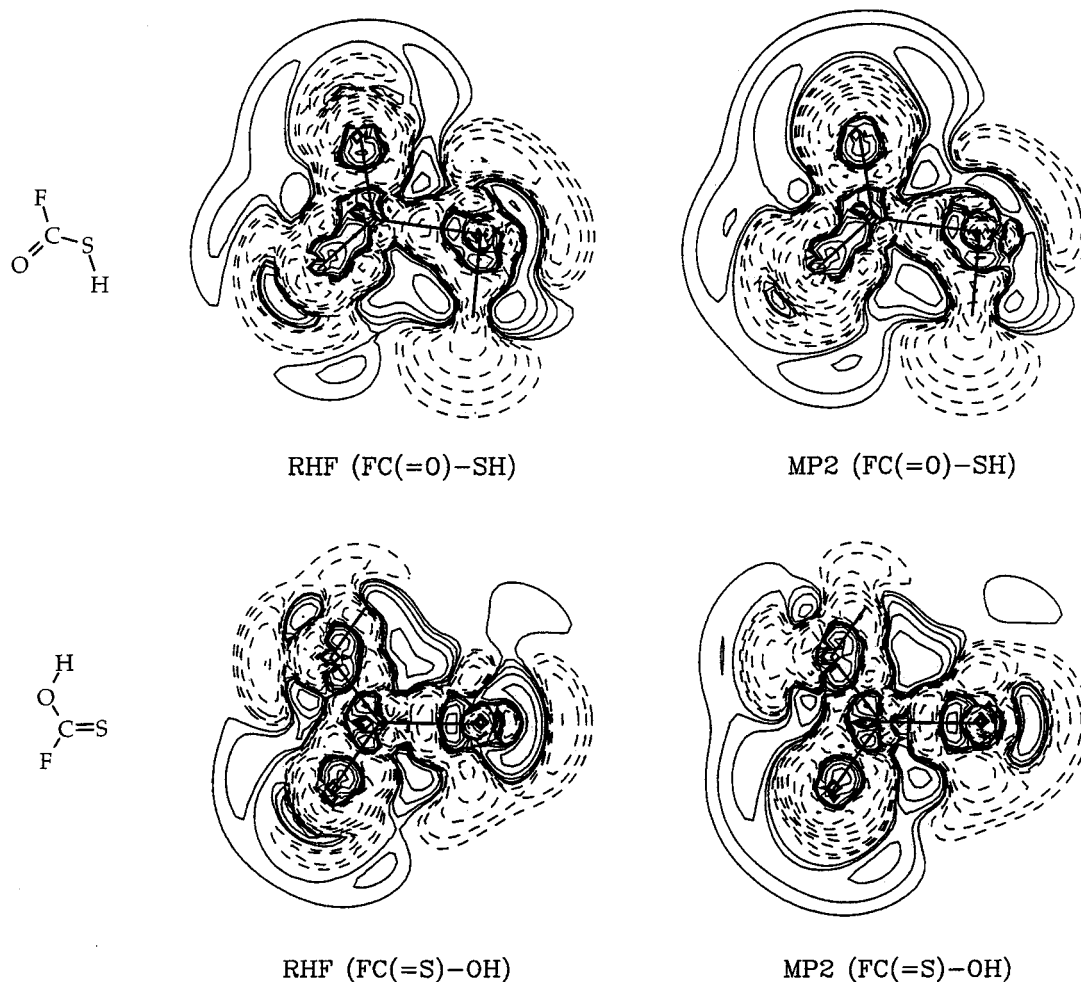


**Figure 3.** Effect of basis set: charge-density-difference plots for the molecular plane ( $\sigma$  system) of  $\text{FC}(=\text{O})-\text{SH}$  and  $\text{FC}(=\text{S})-\text{OH}$ . Left, top: RHF/6-31+G(2d) - RHF/6-31G(d) for  $\text{FC}(=\text{O})-\text{SH}$ . Right, top: MP2/6-31+G(2d) - MP2/6-31G(d) for  $\text{FC}(=\text{O})-\text{SH}$ . Left, bottom: RHF/6-31+G(2d) - RHF/6-31G(d) for  $\text{FC}(=\text{S})-\text{OH}$ . Right, bottom: MP2/6-31+G(2d) - MP2/6-31G(d) for  $\text{FC}(=\text{S})-\text{OH}$ . The outermost contour is 0.0001  $e/b^3$  and increases by a factor of 2 for each successive contour.

C and Y in the C-Y(H) bond. The effect is more dramatic with the highly covalent C-S bond in  $\text{FC}(=\text{O})-\text{SH}$  than with the more polar C-O bond in  $\text{FC}(=\text{S})-\text{OH}$ .

Figures 3 and 4 illustrate the effect of changing the basis set from 6-31G(d) to 6-31+G(2d), defined as the charge density derived from the HF/6-31G(d) wave function subtracted from that derived from the HF/6-31+G(2d) wave function. Figure 3, which depicts the difference density in the plane of the molecule and hence the  $\sigma$  system, clearly shows that the 6-31+G(2d) basis set attempts to place more charge density at the periphery of the molecules, while removing density from the bonding regions between atoms. There is also an accumulation of charge in the region between the C(=Y) and Y-H bonds. The 6-31+G(2d) basis set decreases the amount of charge density at the nuclei.

Figure 4, on the other hand, shows the total difference density, i.e.,  $\sigma$  and  $\pi$  together. For  $\text{FC}(=\text{O})-\text{SH}$ , the 6-31+G(2d) basis set decreases the amount of charge at the nuclei, particularly oxygen and fluorine. It also causes accumulation of charge density in the region between the atoms of the C=O and S-H bonds. With  $\text{FC}(=\text{S})-\text{OH}$ , charge density decreases at the periphery of sulfur and increases in the region closer to carbon and between the atoms of the C=S and O-H bonds. In general, comparisons of Figures 1 and 2 and of Figures

**Table 2.** Difference Density Sums for  $\text{FC}(=\text{O})-\text{SH}$  and  $\text{FC}(=\text{S})-\text{OH}^a$

method	$\text{FC}(=\text{O})-\text{SH}$	$\text{FC}(=\text{S})-\text{OH}$
RHF/6-31+G(2d) - RHF/6-31G(d)	-0.1914	-0.1851
MP2/6-31+G(2d) - MP2/6-31G(d)	-0.2356	-0.2167
MP2/6-31+G(2d) - RHF/6-31+G(2d)	-0.3000	-0.2951

<sup>a</sup> Using the respective MP2/6-31G(d) geometry.

3 and 4 show that the  $\sigma$  and  $\pi$  systems tend to compensate for each other, such that the *total* redistribution of charge is, in some gross sense, always less than that occurring in the  $\sigma$  and  $\pi$  systems separately. This apparent tendency of charge-density changes in the  $\sigma$  and  $\pi$  systems to counteract each other is in complete accord with the observations we have made with a wide variety of other structural motifs.<sup>19,20</sup>

It is also possible to quantify the total extent of charge-density redistribution by integrating the entire difference-density cube in such a way that positive and negative contributions are summed separately. The values obtained in this manner are listed in Table 2. It is readily apparent that changing the level of theory from HF to MP2 at a given basis set induces a larger charge-

(19) Wiberg, K. B.; Rablen, P. R. *J. Am. Chem. Soc.* **1993**, *115*, 9234.  
 (20) Wiberg, K. B.; Rablen, P. R.; Marquez, M. *J. Am. Chem. Soc.* **1992**, *114*, 8654.

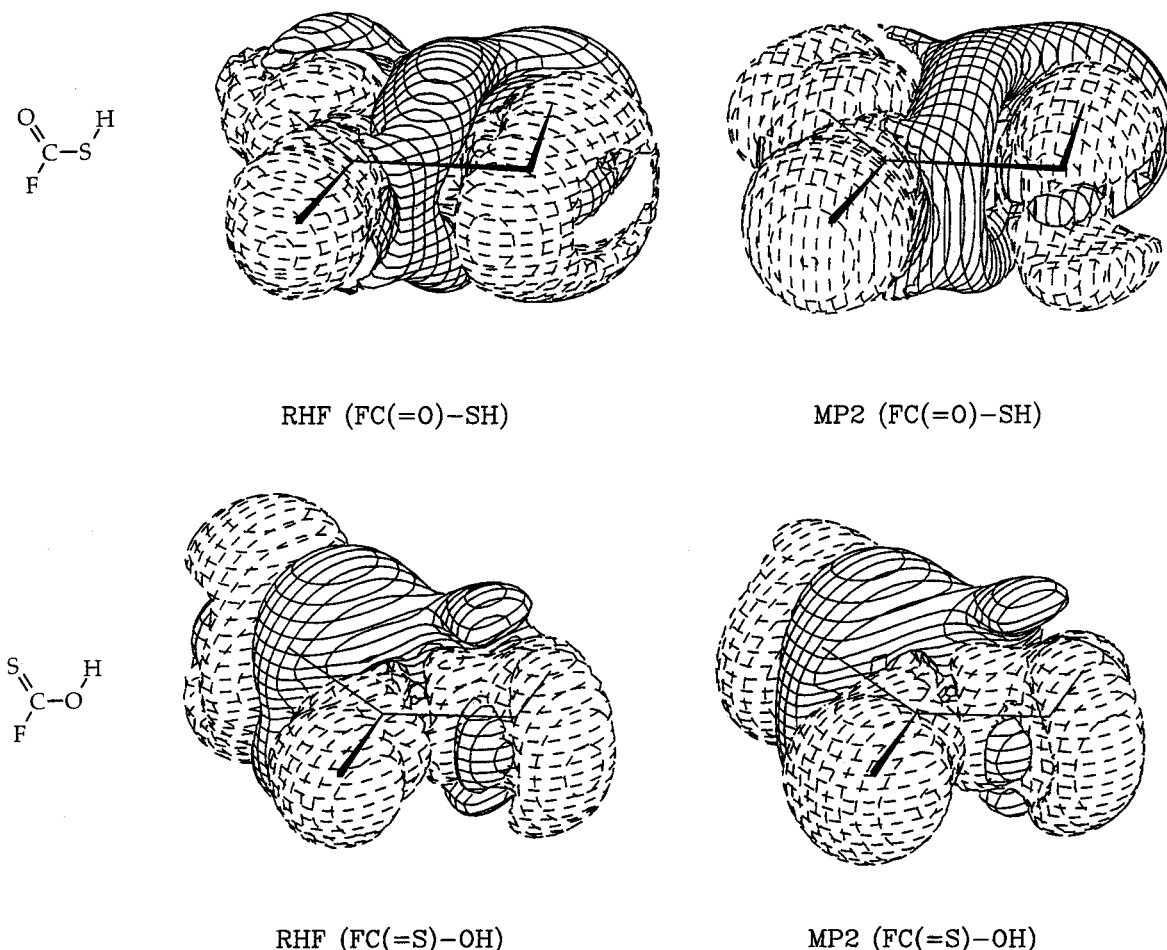
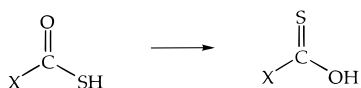


**Figure 4.** Effect of basis set: charge-density-difference plots for the total distribution of  $\text{FC}(=\text{O})\text{-SH}$  and  $\text{FC}(=\text{S})\text{-OH}$ . Left, top: RHF/6-31+G(2d) – RHF/6-31G(d) for  $\text{FC}(=\text{O})\text{-SH}$ . Right, top: MP2/6-31+G(2d) – MP2/6-31G(d) for  $\text{FC}(=\text{O})\text{-SH}$ . Left, bottom: RHF/6-31+G(2d) – RHF/6-31G(d) for  $\text{FC}(=\text{S})\text{-OH}$ . Right, bottom: MP2/6-31+G(2d) – MP2/6-31G(d) for  $\text{FC}(=\text{S})\text{-OH}$ . The outermost contour is  $0.0001 e/b^3$ .

density reorganization than does merely changing the basis set at either the HF or MP2 level of theory. Inclusion of correlation also affects molecular geometry more profoundly than does changing the basis set, at least given that the smaller basis set examined (6-31G(d)) is already of reasonable quality. As a general rule, sulfur is less strongly affected than oxygen by either sort of change in the type of calculation, and bonds to sulfur change to a lesser degree than do bonds to oxygen. This observation seems reasonable in light of the greater importance of electron repulsion for more electronegative, and thus electron-dense, elements.

### 5. Energy Changes

We have had an ongoing interest in how various functional groups interact in a molecule and in the consequences of such interactions for the total molecular energy. As a result, we were particularly curious about how changing the carbonyl oxygen atom to sulfur would affect the stability of the compounds featured in this study. One way to study substituent effects of this sort is to make use of isomerization reactions of the type shown below.



Energies for these isomerization reactions have been calculated at the HF/6-31+G(d), MP2/6-31+G(2d), MP3/6-311++G(2d,p), and CBS-4 levels of theory and are given in Table 3. The HF estimates are significantly different from the others and are unsatisfactory. The remaining methods give quite similar results, and the CBS-4 values are probably the most reliable. We have calculated one comparative value at G-2, and the CBS-4 and G-2 values are in very good agreement with each other. In all cases, it is energetically preferable to have a C=O double bond and a C–S single bond rather than a C=S double bond and a C–O single bond. It is therefore not surprising that the former type of structure is far more prevalent in nature than the latter.

The preference for a C=O over a C=S bond grows larger with increasing electronegativity of the substituents attached to carbon. This is in exact accord with our earlier conclusion that electronegative substituents stabilize carbonyl groups by increasing the C–O polarization and, as a result, the associated internal coulombic stabilization. Whenever two bonds that are polarized in the same direction are centered on the same carbon atom, the charge separation of each bond serves to increase the polarity, and therefore the strength, of the other.<sup>3,21</sup> Electronegative substituents would be predicted to have a much smaller effect on a C=S group than on a C=O

**Table 3. Energy Difference ( $\Delta E$ ) for  $XH_nC(=O)-SH$  to  $XH_nC(=S)-OH$ <sup>a</sup>**

$XH_n$	HF 6-31+G(2d)	MP2(full) 6-31+G(2d)	MP3(fc) 6-311++G(2d,p) <sup>b</sup>	CBS-4	G-2
CH <sub>3</sub>	7.6	4.2	4.8	5.2	4.3
NH <sub>2</sub> (planar)	4.9	3.3	3.4	4.9	
NH <sub>2</sub> (rotated)	11.5	8.0	8.3	9.5	
HO	10.1	7.8	7.6	9.3	
F	13.7	10.8	10.4	11.9	

<sup>a</sup>  $\Delta E$  is in kilocalories per mole, and the scaled HF/6-31+G(2d) zero-point vibrational energy is included. The calculated energy differences are at 0 K. <sup>b</sup> The MP2(full)/6-31+G(2d) geometry was used.

**Table 4. C–O and C–S Bond Dissociation Energies<sup>a</sup>**

$XH_n$	MP2(full) 6-31+G(2d)	MP3(fc) 6-311++G(2d,p) <sup>b</sup>	CBS-4	G-2
C–O BDE for $XH_nC(=O)-OH$				
CH <sub>3</sub>	111.5	99.3	108.3	109.5
NH <sub>2</sub> (planar)	111.2	99.9	108.6	
NH <sub>2</sub> (rotated)	113.7	101.3		
HO	114.8	103.8	109.2	
F	115.6	103.8	111.4	
C–O BDE for $XH_nC(=S)-OH$				
CH <sub>3</sub>	111.7	97.2	103.7	106.2
NH <sub>2</sub> (planar)	106.7	94.2	101.5	
HO	113.3	99.8	107.8	
F	118.8	101.7	108.2	
C–S BDE for $XH_nC(=O)-SH$				
CH <sub>3</sub>	74.2	66.2	75.9	74.3
NH <sub>2</sub> (planar)	74.6	66.6	75.9	
NH <sub>2</sub> (rotated)	79.2	70.0		
HO	80.2	72.2	78.6	
F	81.3	72.5	81.4	
C–S BDE for $XH_nC(=S)-SH$				
CH <sub>3</sub>	78.9	67.9	75.9	75.7
NH <sub>2</sub> (planar)	72.0	62.6	71.9	
HO	79.5	69.0	79.8	
F	84.9	74.9	79.6	

<sup>a</sup> The BDE (0 K) is in kilocalories per mole, and the scaled HF zero-point vibrational energy is included. <sup>b</sup> The MP2(full)/6-31+G(2d) geometry was used.

group, because of the lesser extent of polarization, which is in agreement with our present findings. Abboud and co-workers have come to very similar conclusions regarding carbonyl and thiocarbonyl compounds.<sup>5</sup> On the basis of both experimental and computational data, they have shown that substituents such as fluorine, hydroxy, and amino groups have qualitatively similar effects on the gas-phase basicities of the two classes of compounds but that the changes are more pronounced in the carbonyl series. Their analysis in terms of intramolecular MO interactions leads to predictions very similar to those obtained via our approach based on resonance and electrostatic arguments.<sup>3</sup>

Substituents often lead to interesting changes in bond strengths that can be explored using bond dissociation energies. The estimated dissociation energies for cleaving the C–O and C–S single bonds were obtained at the MP2, MP3, and CBS-4 levels and appear in Table 4. As a calibration with a related compound, the C–C dissociation energy for acetone was calculated from the CBS-4 energies (Table A), which provided an estimated value of 84.1 kcal/mol that may be compared with the G-2 estimate of 83.5 kcal/mol and the observed value, 82.3  $\pm$  0.5 kcal/mol (at 0 K). With acetic acid (Table 4), the estimated C–O bond dissociation energy (BDE) is 108.3

**Table 5. G-2 and CBS-4 Bond Dissociation Energies for O–H and S–H Bonds (kcal/mol)<sup>a</sup>**

bond	G-2 BDE	CBS-4 BDE	exptl <sup>b</sup>
CH <sub>3</sub> O–H	105.0	106.5	104 $\pm$ 1
CH <sub>3</sub> S–H	86.1	86.4	87 $\pm$ 2
CH <sub>3</sub> C(=O)O–H	112.8	114.5	106 $\pm$ 2
CH <sub>3</sub> C(=S)O–H	83.6	83.7	
CH <sub>3</sub> C(=O)S–H	87.8	88.9	
CH <sub>3</sub> C(=S)S–H	79.3 <sup>c</sup>	74.4	
HC(=O)O–H	111.2	110.1	106 $\pm$ 2
HC(=S)O–H	85.2	84.4	
HC(=O)S–H	88.7	89.0	
HC(=S)S–H	80.6	78.7	

<sup>a</sup> The calculated BDEs are at 0 K. <sup>b</sup> Lias, S. G.; Bartmess, J. E.; Liebman, J. F.; Holmes, J. L.; Levin, R. D.; Mallard, W. G. *J. Phys. Chem. Ref. Data* **1988**, *17*, supplement 1. The experimental values are at 298 K. <sup>c</sup> Using the QCISD/6-31+G\* optimized geometry.

kcal/mol, which may be compared with the G-2 estimate of 109.5 kcal/mol and the experimental value of 108.0  $\pm$  0.7 kcal/mol (at 0 K).<sup>22</sup> The CBS-4 procedure has in fact been tested quite extensively and is known to provide reliably accurate BDEs,<sup>16</sup> and so we were not surprised by its accuracy in the current application. The MP2/6-31+G(2d) and MP3/6-311++G(2d,p) energies failed to reproduce the absolute BDEs satisfactorily, although they do exhibit the correct trends with structural changes.

The C–O bond dissociation energies are not strongly affected either by replacing a C=O by a C=S fragment or by changing the substituents attached to the carbonyl group. There is a small increase in BDE with increasing electronegativity of the attached substituent X. The C–S bond dissociation energies have a similar pattern but are approximately 30 kcal/mol smaller than those for the C–O bonds.

It is possible to use the energies reported in Tables 3 and 4 together with the BDEs for O–H and S–H bonds to estimate the relative strengths of C=O and C=S bonds. The required O–H and S–H BDEs have been calculated at the CBS-4 and G-2 levels and are reported in Table 5. The reaction in which CH<sub>3</sub>C(=O)–SH isomerizes to CH<sub>3</sub>C(=S)–OH yields an energy change of +5 kcal/mol (Table 3). This isomerization reaction involves sacrificing a C=O bond, a C–S bond, and an S–H bond in return for a C=S bond, a C–O bond, and an O–H bond. The difference in BDE for a C–S bond as opposed to a C–O bond is 28 kcal/mol (Table 4), while the difference in BDE for an S–H versus an O–H bond in methyl derivatives is 20 kcal/mol (Table 5). Using a

(22) Table 5 contains further (favorable) comparisons between BDEs calculated at the G-2 and CBS-4 levels of theory.

simple bond additivity scheme, then it is possible to conclude that the C=O BDE is roughly 43 kcal/mol greater than the C=S BDE. So, to a good approximation, a C=O bond is stronger than a C=S bond by twice the amount that a C–O bond is stronger than a C–S bond. This tendency for a double bond to have twice the effect of a single bond between the same two elements is in accord with our observations regarding charge distributions, which are discussed in section 7.

Simple bond additivity schemes frequently have ambiguities in regards to which compounds are the appropriate reference and consequently in the interpretation of the quantities derived from such schemes, and the current case is no exception. Table 5 provides the O–H and S–H BDEs for  $\text{CH}_3\text{C}(=\text{O})\text{S}-\text{H}$  and  $\text{CH}_3\text{C}(=\text{S})\text{O}-\text{H}$  specifically, also calculated at the CBS-4 and G-2 levels of theory. There is very good agreement between the available experimental (298 K) and our theoretical values (0 K) for the X–H BDE of  $\text{CH}_3\text{O}-\text{H}$  and  $\text{CH}_3\text{S}-\text{H}$ , but there is less favorable agreement for  $\text{CH}_3\text{C}(=\text{O})\text{O}-\text{H}$  (exptl, 106 kcal/mol; G-2, 113 kcal/mol). Both G-2 and CBS-4 methods are in relative agreement, and this may indicate a slight error in the experimental value for  $\text{CH}_3\text{C}(=\text{O})\text{O}-\text{H}$ . For comparison, the calculated G-2 and CBS-4 BDEs for the formyl and acetyl derivatives are very similar (Table 5). The experimental value for the O–H BDE in  $\text{HC}(=\text{O})\text{O}-\text{H}$  is  $106 \pm 2$  kcal/mol (similar to that for  $\text{CH}_3\text{C}(=\text{O})\text{O}-\text{H}$ ), and the G-2 BDE is calculated to be higher at 111 kcal/mol.

Using the  $\text{CH}_3\text{C}(=\text{O})\text{S}-\text{H}$  and  $\text{CH}_3\text{C}(=\text{S})\text{O}-\text{H}$  compounds as the reference, the difference between S–H and O–H BDEs is not 20 kcal/mol in favor of O–H, as with the methyl derivatives, but rather 5 kcal/mol in favor of the S–H bond. This value then leads to an estimated difference in the strength of C=S and C=O bonds of only 18 kcal/mol in favor of the C=O bond. So, the C=O bond is incontrovertibly stronger than the C=S bond, but it depends on one's perspective exactly by how much. Insofar as the O–H bond of  $\text{CH}_3\text{C}(=\text{S})\text{O}-\text{H}$  seems anomalously weak, presumably as a result of stabilization in the  $\text{CH}_3\text{C}(=\text{S})\text{O}^\bullet$  radical by the sulfur atom, the estimate derived in the previous paragraph on the basis of methyl derivative BDEs is perhaps more in the spirit of the simple bond additivity approach.

In previous studies we have used isodesmic reactions and comparisons of C–X BDEs between methyl and other derivatives in order to understand the differences in bonding that accompany structural change. For instance, we found that the C–X BDEs of acetyl derivatives, when plotted against those of methyl derivatives, gave a slope of  $\sim 1.6$ . This trend was interpreted in terms of cooperatively enhanced polarity, and thus bond strength, in the acetyl series.<sup>3</sup>

As the electronegativity of a substituent deviates from that of carbon, the methyl C–X BDEs increase, because of the greater strength of polar covalent bonds.<sup>23</sup> In the acetyl series, the carbonyl carbon is already polarized. Further polarization by a second electronegative substituent enhances the strength of both the C–X bond and the C=O bond, as both bonds become more polar than they would be in isolation.<sup>3</sup> Electropositive substituents such as a silyl group cause destabilization in acetyl compounds relative to the corresponding methyl com-

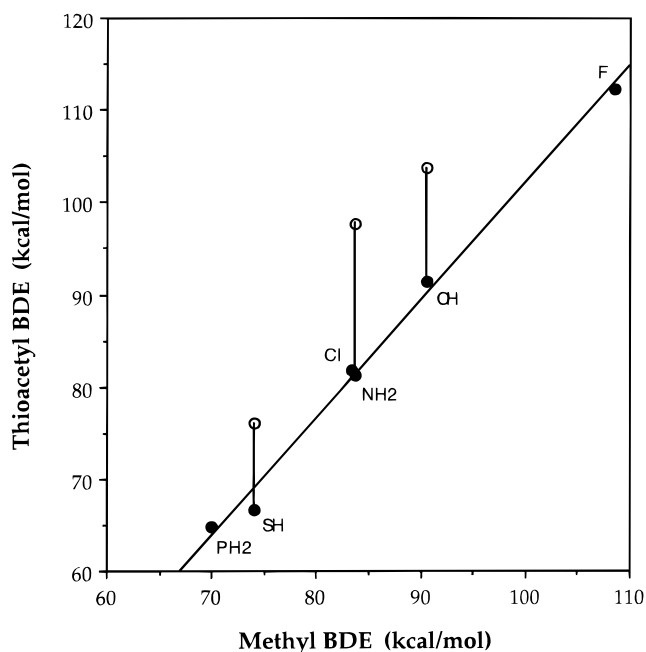


**Figure 5.** Relationship of the CBS-4 C–X bond dissociation energies in the  $\text{CH}_3\text{C}(=\text{S})-\text{X}$  series against the corresponding BDEs for the methyl ( $\text{CH}_3-\text{X}$ ) series. The slope is 1.3, and the correlation coefficient ( $r^2$ ) is 0.994.

**Table 6.** CBS-4 Bond Dissociation Energies of Methyl, Acetyl, and Thioacetyl Derivatives (kcal/mol)<sup>a</sup>

X substituent	$\text{CH}_3-\text{X}$	$\text{CH}_3\text{C}(=\text{O})-\text{X}$	$\text{CH}_3\text{C}(=\text{S})-\text{X}$
NH <sub>2</sub>	83.7	98.2	97.7
NH <sub>2</sub> (TS)		83.8	81.2
OH	90.5	108.3	103.8
OH (TS)		97.0	91.3
F	108.5	120.6	112.2
PH <sub>2</sub>	70.0	61.4	64.8
SH	74.1	75.9	76.1
SH (TS)		67.7	66.7
Cl	83.3	85.4	81.8

<sup>a</sup> The calculated BDEs are at 0 K.

pounds for the same reason. In the vinyl series, on the other hand, bonds are consistently stronger than those in the methyl series because of the change in carbon hybridization, but the amount of increase is essentially constant; i.e., the slope of the plot of vinyl versus methyl BDEs has a value of about 1. This is to be expected since the vinyl group is not polarized in the absence of an electron-withdrawing or electron-donating substituent, and so the effects of electronegativity should parallel those for the methyl series.<sup>19</sup>

To continue our comparison of carbonyl and thiocarbonyl compounds, we have plotted the C–X BDEs (at the CBS-4 level) in the thiocarbonyl (C=S) series against the corresponding methyl C–X BDEs in Figure 5 (Table 6). The correlation is extremely good ( $r^2 = 0.994$ ) when the rotational barriers are subtracted out for the NH<sub>2</sub>, OH, and SH thioacetyl derivatives. In the figure, the solid circles represent the points used to draw the best fit line, while the open circles represent the BDEs prior to subtraction of the rotational barriers. This procedure is chosen to separate the  $\sigma$  and  $\pi$  components of the BDEs and is consistent with the practice used in the previous studies discussed earlier.<sup>3,19</sup> For consistency, the same set of points was used to draw the line in all cases: NH<sub>2</sub>, OH, F, PH<sub>2</sub>, SH, and Cl, with the rotational barriers

(23) Pauling, L. *The Nature of the Chemical Bond*, 2nd ed.; Cornell University Press: Ithaca, NY, 1944.



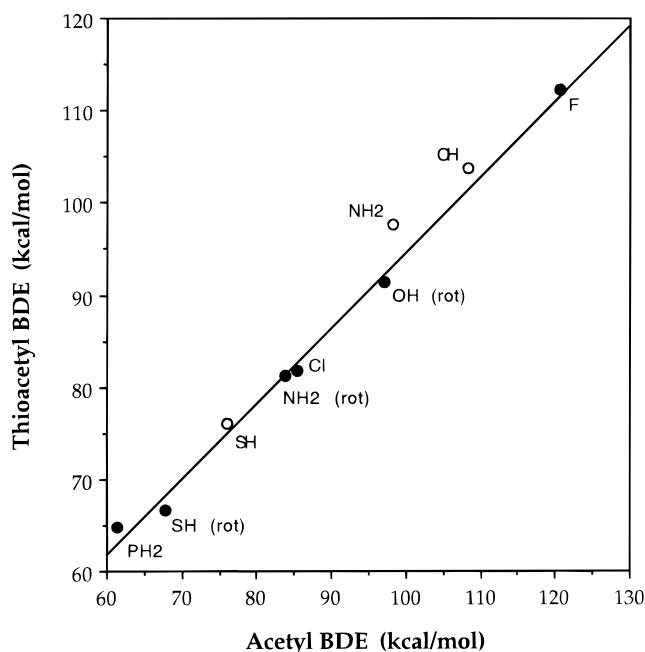


**Figure 6.** Relationship of the CBS-4 C–X bond dissociation energies in the  $\text{CH}_3\text{C}(=\text{S})\text{--X}$  series against the corresponding BDEs for the acetyl ( $\text{CH}_3\text{C}(=\text{O})\text{--X}$ ) series. The slope is 0.8, and the correlation coefficient ( $r^2$ ) is 0.995.

subtracted out for the  $\text{NH}_2$ , OH, and SH derivatives. The coulombic stabilization indicated by the slope (the  $\sigma$  component) should depend primarily on electronegativity and should be independent of the  $\pi$  stabilization of the heteroatom lone pair that is reflected in the rotational barrier.

The slope of Figure 5 is roughly 1.3. This compares with the slope of 1.6 in the case of acetyl–X versus methyl–X derivatives.<sup>3</sup> The smaller slope indicates that there is indeed some coulombic stabilization in thiocarbonyl derivatives of the sort that was observed in the acetyl derivatives. However, as expected because of the reduced polarity of the C=S bond, the magnitude is greatly decreased (closer to unity slope). The same sort of effect should be observable by plotting the BDEs of the thiocarbonyl compounds directly against those of the carbonyl compounds. Figure 6 shows the resulting line, which has a slope of 0.8 and a correlation coefficient ( $r^2$ ) of 0.995. Again, this analysis demonstrates that the thiocarbonyl series is less sensitive to changes in the polarity of the C–X bond than is the carbonyl series but more sensitive than the methyl series or the vinyl series, in accord with its intermediate degree of polarization.

## 6. Acidities

Although our primary focus in this study was on the stability of neutral compounds and on homolytic BDEs, it also seemed worthwhile to explore the acidities of the sulfur-containing analogues of acetic acid. Reliable calculation of gas-phase acidities generally requires accurate treatment of both the neutral and ionic forms of a molecule, and so the computationally expensive but generally applicable G-2 procedure was chosen for this purpose. The absolute energies are available in the Supporting Information (Table B), and the gas-phase acidities ( $\Delta H_{\text{acid}}$ , 0 K) derived from them are listed in Table 7. Gas-phase experimental data (298 K) are

**Table 7.** Gas-Phase Acidities ( $\Delta H_{\text{acid}}$ ) of O–H and S–H Bonds (kcal/mol)<sup>a</sup>

species	G-2 $\Delta H_{\text{acid}}$	exptl <sup>b</sup>
$\text{CH}_3\text{O–H}$	381.4	$381 \pm 2$
$\text{CH}_3\text{S–H}$	356.9	$357 \pm 3$
$\text{CH}_3\text{C}(=\text{O})\text{O–H}$	345.7	$349 \pm 3$
$\text{CH}_3\text{C}(=\text{O})\text{S–H}$	335.8	
$\text{CH}_3\text{C}(=\text{S})\text{O–H}$	331.6	
$\text{CH}_3\text{C}(=\text{S})\text{S–H}$	328.2	
$\text{HC}(=\text{O})\text{O–H}$	342.1	$345 \pm 2$
$\text{HC}(=\text{O})\text{S–H}$	332.2	
$\text{HC}(=\text{S})\text{O–H}$	328.8	
$\text{HC}(=\text{S})\text{S–H}$	325.8	

<sup>a</sup> The calculated acidities are at 0 K; the available experimental values are at 298 K. <sup>b</sup> Lias, S. G.; Bartmess, J. E.; Liebman, J. F.; Holmes, J. L.; Levin, R. D.; Mallard, W. G. *J. Phys. Chem. Ref. Data* **1988**, *17*, supplement 1.

available for the cases of methanol, methanethiol, and acetic acid.<sup>24</sup> The agreement between theory and experiment is reasonable and lends credence to the analysis of structural effects on acidity given below based on the calculated values.

Although OH protons are more acidic than SH protons in aqueous solution, the order is reversed in the gas phase. Presumably, the greater solution acidity of OH protons arises largely from the more favorable solvation energy of the smaller oxygen-centered anions relative to the larger sulfur-centered anions. In the gas phase, however, with no solution stabilization available, the larger size of sulfur relative to oxygen reduces the electrostatic repulsion in the anion and thereby increases the acidity of sulfur compounds.

In the series  $\text{CH}_3\text{C}(=\text{O})\text{--OH}$ ,  $\text{CH}_3\text{C}(=\text{O})\text{--SH}$ ,  $\text{CH}_3\text{C}(=\text{S})\text{--OH}$ , and  $\text{CH}_3\text{C}(=\text{S})\text{--SH}$ , the acidity appears to increase roughly in proportion to the number of sulfur atoms present. The substitution of both oxygens with sulfur results in an increase in acidity (17 kcal/mol) that is considerably less than the increase in acidity on going from methanol to methyl thiol (24 kcal/mol). If the greater size of sulfur is important in enhancing the gas-phase acidity of SH bonds via electrostatic stabilization of the anion, as postulated above, this result makes sense. Substituting oxygen with sulfur should have a more pronounced effect when all of the charge is (formally) concentrated on a single atom, as in methoxide anion and its sulfur analogue, than when it is distributed over two atoms, as in the acetate anion and its sulfur analogues. A saturation effect is also apparent in that the first sulfur substitution into acetic acid to give  $\text{CH}_3\text{C}(=\text{O})\text{--SH}$  yields a larger increase in acidity (10 kcal/mol) than does the second substitution (7 kcal/mol).

Acetic acid has a much greater acidity than methanol because of the delocalized nature of the acetate anion. There has been considerable debate as to whether the stabilization of the carboxylate anion results from a *bona fide* resonance effect or from simple electrostatics.<sup>25,26</sup> It is interesting to note, in the current context, that the enhancement of acidity on going from methanol to acetic acid (35 kcal/mol) is somewhat greater than that obtained on going from  $\text{CH}_3\text{SH}$  to  $\text{CH}_3\text{C}(=\text{S})\text{--SH}$  (29 kcal/mol). Whatever the source of stabilization, it is modestly reduced in strength for sulfur relative to oxygen.

(24) Gal, J.-F.; Maria, P.-C. *Prog. Phys. Org. Chem.* **1990**, *17*, 159–238; p 175.

(25) Wiberg, K. B.; Ochterski, J.; Streitwieser, A. *J. Am. Chem. Soc.* **1996**, *118*, 8291.

**Table 8.** Atomic Charges of  $\text{XH}_n\text{C}(=\text{Y})-\text{YH}$  (MP2/6-31G(d))<sup>a</sup>

compound	C	=Y	–Y–	H	X	$\Sigma\text{XH}_n$
$\text{CH}_3\text{C}(=\text{O})-\text{OH}$	1.6270	-1.2064	-1.1569	0.5934	-0.0678	0.1463
$\text{CH}_3\text{C}(=\text{O})-\text{SH}$	0.9687	-1.1426	-0.0356	0.0781	-0.0914	0.1267
$\text{CH}_3\text{C}(=\text{S})-\text{OH}$	0.1221	0.2606	-1.1386	0.5956	-0.0511	0.1619
$\text{CH}_3\text{C}(=\text{S})-\text{SH}$	-0.6083	0.3259	0.0663	0.0784	-0.0633	0.1402
$\text{NH}_2\text{C}(=\text{O})-\text{OH}$ (pl)	2.1991	-1.2529	-1.1638	0.6015	-1.3160	-0.3930
$\text{NH}_2\text{C}(=\text{O})-\text{SH}$ (pl)	1.5292	-1.1967	-0.0379	0.0861	-1.2997	-0.3845
$\text{NH}_2\text{C}(=\text{S})-\text{OH}$ (pl)	0.8047	0.1081	-1.1545	0.6086	-1.3014	-0.3643
$\text{NH}_2\text{C}(=\text{S})-\text{SH}$ (pl)	0.0467	0.1766	0.0412	0.0937	-1.2814	-0.3605
$\text{NH}_2\text{C}(=\text{O})-\text{OH}$ (rot)	2.0232	-1.2177	-1.1400	0.5937	-1.0585	-0.2553
$\text{NH}_2\text{C}(=\text{O})-\text{SH}$ (rot)	1.2872	-1.1572	0.0755	0.0622	-1.0740	-0.2672
$\text{NH}_2\text{C}(=\text{S})-\text{OH}$ (rot)	0.5226	0.2357	-1.1163	0.5959	-1.0535	-0.2385
$\text{NH}_2\text{C}(=\text{S})-\text{SH}$ (rot)	-0.2692	0.3073	0.1467	0.0616	-1.0611	-0.2501
$\text{HOC}(=\text{O})-\text{OH}$	2.3370	-1.2459	-1.1527	0.6060	-1.1527	-0.5467
$\text{HOC}(=\text{O})-\text{SH}$	1.5638	-1.1950	0.0994	0.0778	-1.1443	-0.5416
$\text{HOC}(=\text{S})-\text{OH}$	0.8749	0.1804	-1.1393	0.6115	-1.1393	-0.5278
$\text{HOC}(=\text{S})-\text{SH}$	0.0354	0.2619	0.1492	0.0796	-1.1281	-0.5238
$\text{FC}(=\text{O})-\text{OH}$	2.3959	-1.2076	-1.1451	0.6126	-0.6514	-0.6514
$\text{FC}(=\text{O})-\text{SH}$	1.5600	-1.1583	0.1579	0.0837	-0.6409	-0.6409
$\text{FC}(=\text{S})-\text{OH}$	0.8314	0.3364	-1.1342	0.6150	-0.6466	-0.6466
$\text{FC}(=\text{S})-\text{SH}$	-0.0355	0.4159	0.1759	0.0817	-0.6368	-0.6368

<sup>a</sup> With the optimized MP2/6-31G(d) geometry for each compound.

It is also interesting to note that while the acetate anion and its dithio analogue both experience strong stabilization as a result of delocalization, the acetoxy radical does not. Examination of the calculated BDEs in Table 5 reveals that the homolytic BDE for the O–H bond of acetic acid is considerably *greater* than that for methanol! The enhanced bond strength can be rationalized on the basis of the greater polarity of the O–H bond in acetic acid compared to that in methanol. Apparently, however, stabilization of the acetoxy radical by delocalization is modest at best and does not result in a decreased O–H BDE for the conjugated system. In at least an anecdotal sense, this observation suggests that the primary source of stabilization in the acetate anion is electrostatic, i.e., the reduced concentration of net charge, and not electron delocalization per se. The dithio analogue of the acetoxy radical, on the other hand, *does* appear to experience substantial stabilization, as demonstrated by the *lower* BDE for the S–H bond of  $\text{CH}_3\text{C}(=\text{S})-\text{SH}$  (74.4 kcal/mol) as compared to  $\text{CH}_3\text{SH}$  (86.4 kcal/mol).

## 7. Charge Distributions and Bond Orders

We have held a long-standing interest in charge distributions in molecules and, therefore, wished to examine the differences in charge distribution among the compounds included in this investigation. Atomic charges were calculated according to Bader's theory of atoms in molecules by integrating the charge distribution within properly defined atomic domains,<sup>27</sup> and the populations thus obtained were converted into charges by subtracting

them from the nuclear charges. The values are given in Table 8. This analysis also leads to an atomic overlap matrix from which the covalent bond orders may be calculated according to the procedure of Cioslowski.<sup>14</sup> These quantities are given in Table 9.

The calculated charges may appear to be quite large in some cases. They represent the first term of an expansion that includes atomic dipoles, quadrupoles, and so on, which result from the charge distribution of an atom not being distributed symmetrically with respect to the nucleus. However, the *changes* in values are the important quantities in comparing the compounds. As part of a published comparison of the different partitioning methods available for calculating atomic charges, we have shown that even when different definitions yield drastically varying atomic charges, they frequently provide a consistent picture of how atomic charges *change* in response to molecular structure.<sup>28</sup>

In the examination of acetic acid and its sulfur-substituted derivatives, it is readily apparent that the charge at the carbonyl carbon decreases as the number of oxygens is decreased. This result is expected since oxygen is considerably more electronegative than carbon, whereas sulfur has about the same electronegativity as carbon. The comparison between  $\text{CH}_3\text{C}(=\text{S})-\text{OH}$  and  $\text{CH}_3\text{C}(=\text{O})-\text{SH}$  is particularly enlightening. In both cases, the number of oxygen and sulfur atoms attached to the carbon is the same. However, the charge at carbon is quite different! *It appears that in its interaction with carbon a double bond to oxygen behaves in a fashion equivalent to two single bonds.* The charge at carbon in the series  $\text{CH}_3\text{C}(=\text{O})-\text{OH}$  ( $N_0 = 3$ ),  $\text{CH}_3\text{C}(=\text{O})-\text{SH}$  ( $N_0 = 2$ ),  $\text{CH}_3\text{C}(=\text{S})-\text{OH}$  ( $N_0 = 1$ ),  $\text{CH}_3\text{C}(=\text{S})-\text{SH}$  ( $N_0 = 0$ ) *does* correlate very closely with the total number of C–O bonds: the equation of the line is

$$\text{charge at carbon} = -0.606 + 0.755N_0$$

with a correlation coefficient of 0.998, where  $N_0$  is the number of bonds to oxygen.

The polar nature of the C=O group is seen in the covalent bond orders (Table 9), where the values are on

(26) Ji, D.; Thomas, D. *J. Phys. Chem.* **1994**, *98*, 4301. Perrin, C. L. *J. Am. Chem. Soc.* **1991**, *113*, 2865. Taft, R. W.; Koppel, I. A.; Topsom, R. D.; Anvia, F. *J. Am. Chem. Soc.* **1990**, *112*, 2047. Dewar, M. J. S.; Krull, K. *J. Chem. Soc., Chem. Commun.* **1990**, 333. Martin, G. *Tetrahedron Lett.* **1990**, *31*, 5181. Thomas, T. D.; Carroll, T. X.; Siggel, M. R. F. *J. Org. Chem.* **1988**, *53*, 1812. Thomas, T. D.; Siggel, M. R. F.; Streitwieser, A., Jr. *J. Mol. Struct. (THEOCHEM)* **1988**, *165*, 309. Siggel, M. R. F.; Streitwieser, A., Jr.; Thomas, T. D. *J. Am. Chem. Soc.* **1988**, *110*, 8022. Exner, O. *J. Org. Chem.* **1988**, *53*, 1812. Wiberg, K. B.; Laidig, K. *J. Am. Chem. Soc.* **1987**, *109*, 5935. Siggel, M. R.; Thomas, T. D. *J. Am. Chem. Soc.* **1986**, *108*, 4360.

(27) (a) Bader, R. F. W. *Atoms in Molecules. A Quantum Theory*; Clarendon Press: Oxford, 1990. (b) Bader, R. F. W. *Acc. Chem. Res.* **1985**, *18*, 9. (c) Bader, R. F. W. *Chem. Rev.* **1991**, *91*, 893.

(28) Wiberg, K. B.; Rablen, P. R. *J. Comput. Chem.* **1993**, *14*, 1504.

**Table 9.** Covalent Bond Orders of  $\text{XH}_n\text{C}(=\text{Y})\text{-ZH}$  (MP2/6-31G(d))<sup>a</sup>

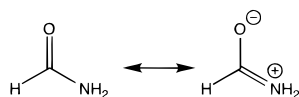
$\text{XH}_n\text{C}(=\text{Y})\text{-ZH}$	C=Y		C-Y		Z-H		C-X		X-H <sub>a</sub>	X-H <sub>b</sub>
	$\pi$	total	$\pi$	total	$\pi$	total	$\pi$	total	total	total
$\text{CH}_3\text{C}(=\text{O})\text{-OH}$	0.531	1.242	0.207	0.821	0.012	0.603	0.046	0.992	0.946	0.937
$\text{CH}_3\text{C}(=\text{O})\text{-SH}$	0.614	1.394	0.214	1.144	0.047	1.003	0.043	0.996	0.942	0.936
$\text{CH}_3\text{C}(=\text{S})\text{-OH}$	0.785	1.879	0.264	0.977	0.011	0.590	0.068	0.987	0.943	0.932
$\text{CH}_3\text{C}(=\text{S})\text{-SH}$	0.856	1.959	0.262	1.250	0.043	0.991	0.069	1.019	0.938	0.935
$\text{NH}_2\text{C}(=\text{O})\text{-OH (pl)}$	0.441	1.137	0.166	0.757	0.012	0.597	0.251	0.930	0.759	0.756
$\text{NH}_2\text{C}(=\text{O})\text{-SH (pl)}$	0.512	1.269	0.170	1.090	0.049	1.001	0.290	1.014	0.754	0.760
$\text{NH}_2\text{C}(=\text{S})\text{-OH (pl)}$	0.637	1.694	0.218	0.886	0.011	0.578	0.348	1.078	0.743	0.750
$\text{NH}_2\text{C}(=\text{S})\text{-SH (pl)}$	0.731	1.813	0.219	1.168	0.045	0.986	0.379	1.176	0.741	0.757
$\text{NH}_2\text{C}(=\text{O})\text{-OH (rot)}$	0.509	1.203	0.216	0.804	0.012	0.604	0.062	0.915	0.799	
$\text{NH}_2\text{C}(=\text{O})\text{-SH (rot)}$	0.595	1.356	0.247	1.191	0.046	1.004	0.067	0.951	0.796	
$\text{NH}_2\text{C}(=\text{S})\text{-OH (rot)}$	0.763	1.845	0.282	0.957	0.011	0.591	0.079	0.995	0.789	
$\text{NH}_2\text{C}(=\text{S})\text{-SH (rot)}$	0.843	1.957	0.296	1.265	0.042	0.995	0.081	1.038	0.790	
$\text{HOC}(=\text{O})\text{-OH}$	0.446	1.133	0.182	0.760	0.012	0.594	0.182	0.760	0.594	
$\text{HOC}(=\text{O})\text{-SH}$	0.525	1.271	0.209	1.136	0.047	0.998	0.212	0.848	0.593	
$\text{HOC}(=\text{S})\text{-OH}$	0.679	1.747	0.243	0.899	0.011	0.578	0.243	0.899	0.578	
$\text{HOC}(=\text{S})\text{-SH}$	0.775	1.885	0.259	1.207	0.043	0.989	0.261	0.990	0.581	
$\text{FC}(=\text{O})\text{-OH}$	0.473	1.165	0.191	0.773	0.011	0.587	0.122	0.637		
$\text{FC}(=\text{O})\text{-SH}$	0.556	1.318	0.233	1.167	0.045	0.993	0.137	0.715		
$\text{FC}(=\text{S})\text{-OH}$	0.746	1.836	0.249	0.907	0.010	0.575	0.154	0.749		
$\text{FC}(=\text{S})\text{-SH}$	0.828	1.975	0.267	1.223	0.043	0.987	0.159	0.829		

<sup>a</sup> Using the optimized MP2/6-31G(d) geometry for each compound.

the order of 1.2 for C=O as compared with 1.8–1.9 for C=S. The electronegativity of oxygen is also evident in its bonds to hydrogen, as the O–H covalent bond order is about 0.6 as compared to about 1.0 for S–H bonds.

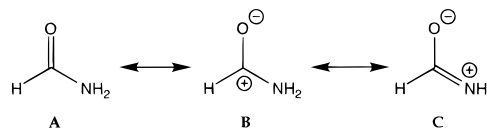
### 8. Charge Transfer during Bond Rotation

The high barrier to C–N bond rotation in amides has been attributed in the past to energetically stabilizing charge transfer from the nitrogen lone pair into the carbonyl  $\pi$  system, which is possible in the ground-state (planar) conformer but not in the rotational transition states. This charge transfer has traditionally been described in terms of the resonance structures shown below, which imply that charge transfer occurs primarily from nitrogen to oxygen.<sup>29</sup>



However, it has been shown that the charge distribution around the carbonyl oxygen changes very little during C–N bond rotation in amides and that the  $\pi$  charge density donated by the nitrogen lone pair is transferred to carbon rather than oxygen.<sup>7,30</sup> This phenomenon can be described in terms of a modified resonance picture by stating that the contribution of the resonance structure with the C=N double bond (C) increases at the expense of the dipolar C<sup>+</sup>–O<sup>–</sup> structure (B) rather than of the canonical C=O structure (A) for the overall character of the “resonance hybrid.”

Atomic charges have frequently been used in the past to quantify charge transfer during conformational changes,<sup>6,17b,28,31</sup> but the model-dependent definition of atomic charge can be circumvented by directly examining



the change in the molecular charge density distribution. This is most easily accomplished by subtracting the charge-density distribution of the ground-state conformer from that of the transition state for bond rotation.<sup>7,19</sup> The resulting difference density shows where charge density flows upon going from the ground state to the transition state.

In the regions where atoms are actually moving, e.g., the amino group for formamide, the creation and annihilation of atoms in different positions dominates the difference density. It is difficult to make sense of these changes, and they are generally deleted so as to clarify the changes in other regions. Where the atoms do not move, however, such as in the formyl group of formamide, the difference density faithfully describes the charge transfer. It is necessary to constrain the region of interest, e.g., in this case the formyl group, to maintain the same geometry in the ground and transition states in order to obtain a reliable difference. However, this constraint generally has a very small energetic cost and should not cause any significant distortions in the results. Difference-density maps of this sort have been used to demonstrate that, contrary to conventional intuition, the charge transfer to the terminal oxygen of acetamide is less than that to the terminal methylene of vinylamine during the C–N bond rotation process.<sup>19</sup>

We have used the same technique here to observe the charge transfer occurring during C–N, C–O, and C–S bond rotation in the species  $\text{NH}_2\text{C}(=\text{O})\text{OH}$ ,  $\text{NH}_2\text{C}(=\text{O})\text{SH}$ ,  $\text{NH}_2\text{C}(=\text{S})\text{OH}$ , and  $\text{NH}_2\text{C}(=\text{S})\text{SH}$ . The resulting difference-density maps are shown in Figures 7 and 8, where the surfaces represent the 0.002 e/b<sup>3</sup> contour. Solid lines represent positive values and indicate greater charge density in the rotated transition state as compared to that in the ground state, while dashed contours represent negative difference densities and, hence, indicate regions with greater charge density in the ground state than in

(29) Wheland, G. W. *Resonance in Organic Chemistry*; John Wiley & Sons: New York, 1955; p 109.

(30) Wiberg, K. B.; Breneman, C. M. *J. Am. Chem. Soc.* **1992**, *114*, 831.

(31) Wiberg, K. B.; Hadad, C. M.; Breneman, C. M.; Laidig, K. E.; Murcko, M. A.; LePage, T. L. *Science* **1991**, *252*, 1266.

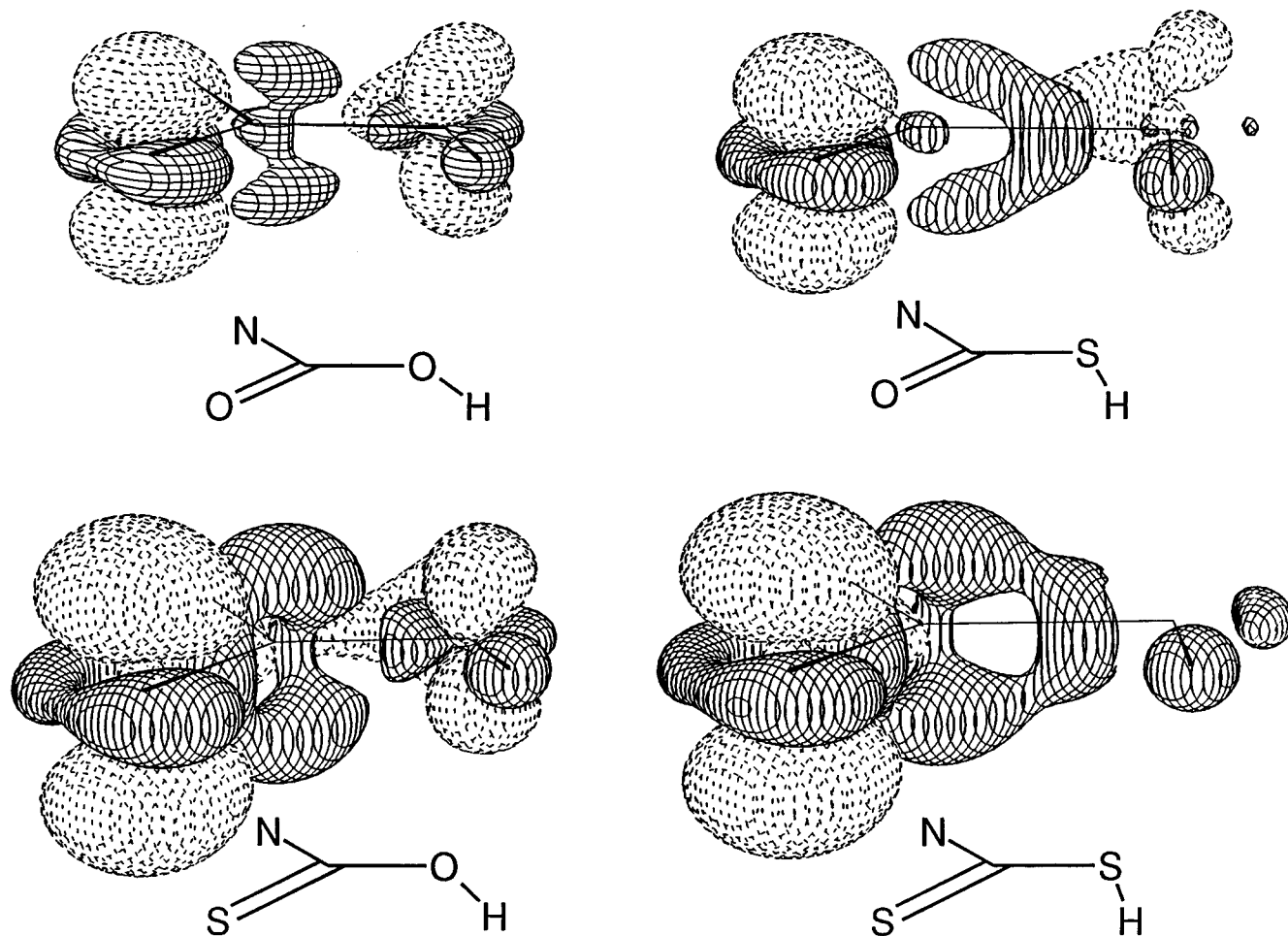


**Figure 7.** Difference density that occurs during C–N bond rotation in  $\text{NH}_2\text{C}(=\text{O})\text{--OH}$ ,  $\text{NH}_2\text{C}(=\text{O})\text{--SH}$ ,  $\text{NH}_2\text{C}(=\text{S})\text{--OH}$ , and  $\text{NH}_2\text{C}(=\text{S})\text{--SH}$  at the  $0.002 e/b^3$  contour. Solid lines indicate greater charge density in the rotated transition state as compared to that in the ground state. The regions of difference density in the immediate vicinity of the moving  $\text{NH}_2$  group have been removed to provide a clearer picture.

**Table 10.** MP2(fc)/6-31+G(d) Integrated Charge Shifts for C–N, C–O, and C–S Rotation

compound	C–N rotation			C–O or C–S rotation		
	$\sigma$	$\pi$	total	$\sigma$	$\pi$	total
$\text{NH}_2\text{C}(=\text{O})\text{--OH}$	+0.027	–0.054	–0.027	+0.012	–0.034	–0.022
$\text{NH}_2\text{C}(=\text{O})\text{--SH}$	+0.030	–0.061	–0.031	+0.011	–0.025	–0.014
$\text{NH}_2\text{C}(=\text{S})\text{--OH}$	+0.036	–0.095	–0.059	+0.019	–0.054	–0.035
$\text{NH}_2\text{C}(=\text{S})\text{--SH}$	+0.049	–0.108	–0.059	+0.018	–0.046	–0.028

the transition state. In all cases, the region of difference density in the immediate vicinity of the moving group ( $\text{NH}_2$ , SH, or OH) has been removed to provide a clearer picture. The carbonyl oxygen ( $=\text{O}$ ) or thiocarbonyl sulfur ( $=\text{S}$ ) is the region of greatest interest.

In general, Figure 7 shows that amino group rotation has an effect in these compounds similar to that in acetamide or vinylamine.<sup>19</sup> The ground state shows greater charge density in the  $\pi$  region of the carbonyl oxygen or thiocarbonyl sulfur than does the transition state, as indicated by the dashed pair of regions which roughly resemble a  $\pi$  orbital. One can understand this shift in terms of the traditional molecular orbital arguments or as the tendency to decrease electron–electron repulsion in the high-density region of the nitrogen lone pair via delocalization into the somewhat less densely charged region of the  $\text{C}=\text{O}$  or  $\text{C}=\text{S}$   $\pi$  system. In each case, there is also a region of opposite polarity in the plane of the molecule, representing reduced charge

density for the ground state with respect to the transition state. It is reasonable that if charge density flows to the  $\pi$  region of the terminal oxygen or sulfur, electron–electron repulsion will increase substantially unless some charge density flows in the reverse direction in the  $\sigma$  system. This sort of  $\sigma/\pi$  polarization is generally neglected in simple models that emphasize the  $\pi$  system, such as classical resonance theory or Hückel theory. However, it is frequently observed and has important consequences.<sup>7,19,20,32</sup>

While similar in broad features, the difference-density plots for the various compounds in Figures 7 and 8 nonetheless differ quantitatively (Table 10). Considering first the plots corresponding to C–N rotation in Figure 7, the amount of charge transfer to sulfur in  $\text{NH}_2\text{C}(=\text{S})\text{OH}$  and  $\text{NH}_2\text{C}(=\text{S})\text{SH}$  is much greater than that to oxygen

(32) Wiberg, K. B.; Rosenberg, R. E.; Rablen, P. R. *J. Am. Chem. Soc.* **1991**, *113*, 2890.

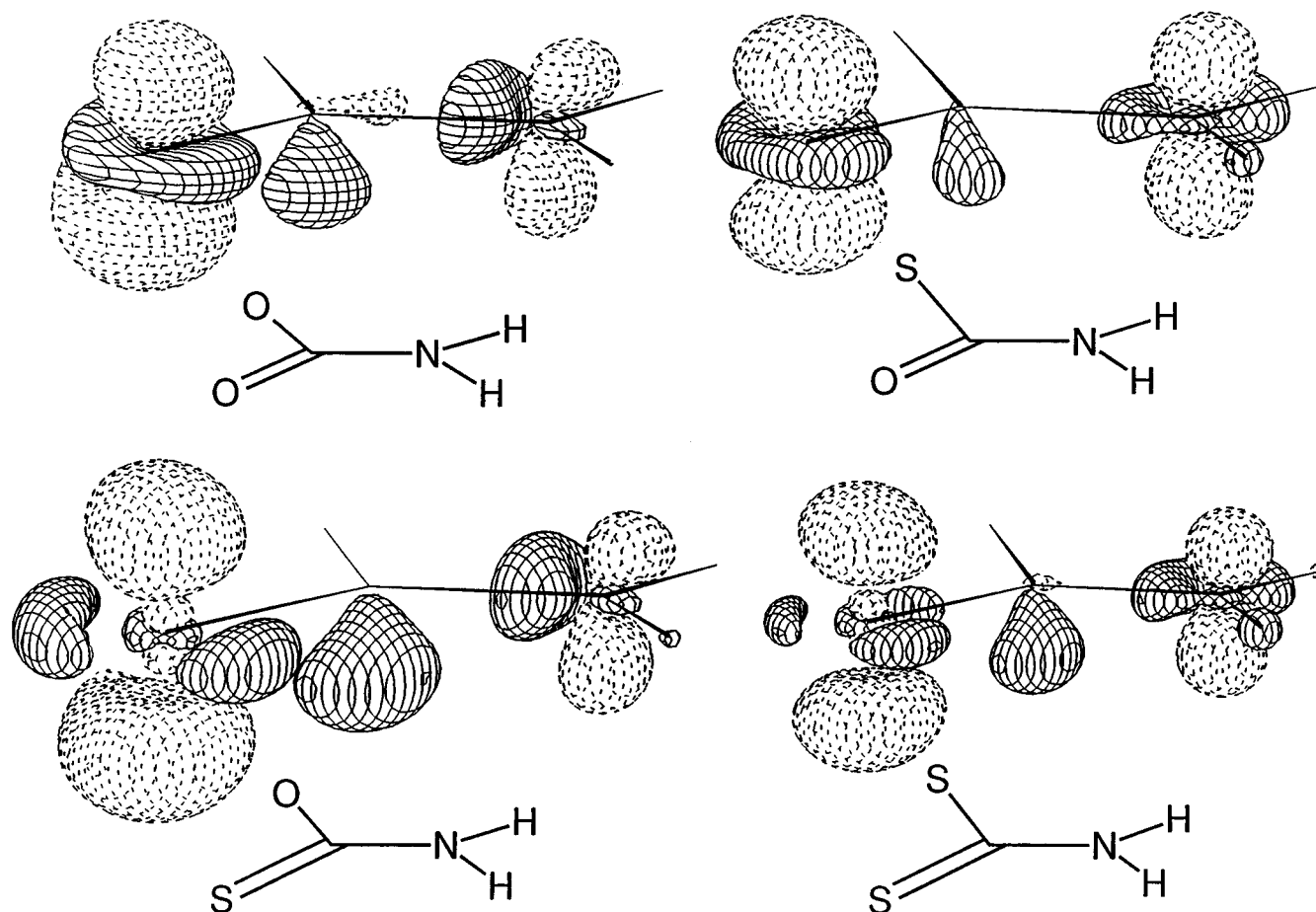


**Figure 8.** Difference density that occurs during C–O and C–S bond rotations in  $\text{NH}_2\text{C}(=\text{O})\text{--OH}$ ,  $\text{NH}_2\text{C}(=\text{O})\text{--SH}$ ,  $\text{NH}_2\text{C}(=\text{S})\text{--OH}$ , and  $\text{NH}_2\text{C}(=\text{S})\text{--SH}$  at the  $0.002 \text{ e/b}^3$  contour. Solid lines indicate greater charge density in the rotated transition state as compared to that in the ground state. The regions of difference density in the immediate vicinity of the moving SH or OH groups have been removed to provide a clearer picture.

in  $\text{NH}_2\text{C}(=\text{O})\text{OH}$  and  $\text{NH}_2\text{C}(=\text{O})\text{SH}$ . The differences *between* the members of each of these two groups, on the other hand, seem to be minor, at least in the region of the doubly bonded atom. It appears that sulfur, being more polarizable than oxygen and having less negative charge, has a much greater ability to accept charge density from the nitrogen lone pair than does oxygen. The enhanced ability of the thiocarbonyl group to accept a  $\pi$  charge donated by a substituent at the carbon position is in accord with the behavior of thioamides in comparison to amides. Thioamides have C–N rotational barriers somewhat greater than those for amides, and the bond rotation process causes about twice as much polarization of the C=S bond in thioamides as of the C=O bond in amides.<sup>7,33</sup> It has been noted before that the thiocarbonyl (C=S) group interacts to a greater extent with strongly electron-donating substituents than does the carbonyl (C=O) group.<sup>34</sup>

Integrating the  $\sigma$  and  $\pi$  charge densities in the regions near the carbonyl and thiocarbonyl groups makes the discussion of charge transfer somewhat more quantitative. Using a methodology described in the computational methods section, the volumes corresponding to the positive and negative regions in the difference-density

plots were integrated. The regions in the molecular plane are referred to as  $\sigma$ , while the ones above and below the plane are combined and referred to as  $\pi$ . The results are listed in Table 10 and support the qualitative analyses of the difference-density plots. For instance, on average C–N rotation results in almost twice as much total charge transfer to sulfur (0.059 e) as to oxygen (average of 0.029 e). In addition, the  $\sigma$  and  $\pi$  systems show opposite trends; that is, a transfer of charge in the  $\pi$  system is always partially offset by an opposite movement of charge in the  $\sigma$  system.

An explanation of the greater charge transfer to sulfur can also be made in terms of molecular orbital arguments. The N lone pair interacts with the C=S or C=O  $\pi^*$  orbital, causing charge density to reside in the latter and leading to stabilization of the planar ground state. The C=O  $\pi$  bond is highly polarized toward the oxygen; therefore, the  $\pi^*$  orbital should be highly polarized toward the carbon. Thus, one would expect the charge density contributed by the nitrogen lone pair to go mostly to the carbonyl carbon or the region between carbon and nitrogen rather than to oxygen. This insight is often neglected in the simple resonance explanation. Sulfur, on the other hand, has an electronegativity similar to that of carbon, and so both the  $\pi$  and  $\pi^*$  orbitals are relatively unpolarized. Consequently, a large fraction of the charge density contributed by nitrogen should end up on sulfur. This analysis agrees with the much larger

(33) (a) Lee, C. M.; Kumler, W. D. *J. Org. Chem.* **1962**, *27*, 2052. (b) Jensen, K. A. *Acta Chem. Scand.* **1963**, *17*, 551.

(34) Lüttringhaus, A.; Grohmann, J. *Z. Naturforsch.* **1955**, *10b*, 365.

difference density around sulfur in the C=S species than around the oxygen in the C=O species.

Turning now to the difference densities for C–O and C–S rotation (Figure 8), the plots are no longer symmetric since the C–OH and C–SH bond rotation processes, unlike the C–NH<sub>2</sub> rotation processes, break the C<sub>s</sub> symmetry of the molecules. Aside from the loss of symmetry, the other major change from the first set of plots is the smaller size and integrations of the charge-transfer regions. The lone pairs of oxygen and sulfur are less basic than those of nitrogen, and consequently, they are weaker  $\pi$  donors. The smaller integrations in Table 10 are in accord with this expectation. Furthermore, visual inspection reveals that the regions for C–S rotation are slightly, but noticeably, smaller than those for C–O rotation. Based on the tabulated integrations, the average total charge transfer for C–S rotation is 0.021 e, while that for C–O rotation is 0.029 e. Apparently the lone pairs of sulfur are somewhat less able to polarize the C=O and C=S  $\pi$  systems than are the lone pairs of oxygen. This observation demonstrates that more than just electronegativity is involved in determining  $\pi$ -donating power. If electronegativity were the only important factor, oxygen would indeed be a weaker donor than nitrogen, but sulfur would be the strongest donor. The fact that sulfur is instead the weakest donor shows that size and polarizability, or possibly other factors, must play an important role. The lone pairs of sulfur might be too diffuse and weakly bound, i.e., soft,<sup>35</sup> to polarize the (hard) C=O bond; it is easier to polarize the sulfur lone pair instead.

Finally, Figure 8 also shows that charge reorganization is always greater in the thiocarbonyl compound (to C=S) than in its carbonyl counterpart (to C=O). This observation is consistent with the arguments made above for C–N rotation. The ratio is slightly less than the factor of 2 observed with C–N rotation, with an average transfer to oxygen of 0.018 e and an average transfer to sulfur of 0.032 e.

## 9. Conclusions

The XH<sub>n</sub>C(=Y)–YH series of compounds, where XH<sub>n</sub> = CH<sub>3</sub>, NH<sub>2</sub>, HO, and F and Y = O and S, were examined via *ab initio* molecular orbital calculations. Systematic

comparisons show that C=O bonds are stronger than C=S bonds and that XH<sub>n</sub>C(=O)–SH is thermodynamically preferable to XH<sub>n</sub>C(=S)–OH. The charge-density analysis confirms that a C=S fragment is very close to a covalent double bond, while the C=O bond has very significant polar (C<sup>+</sup>–O<sup>-</sup>) character. This polarized character of C=O bonds provides a significant portion of their unusual strength. Also, in its interaction with carbon, a double bond to oxygen behaves in a fashion equivalent to two single bonds, and there is a large positive charge on the carbonyl carbon as a result.

Charge-density-difference plots were obtained at the MP2/6-31+G(d) level to investigate the nature of electronic reorganization resulting from rotation about the C–NH<sub>2</sub>, C–OH, and C–SH bonds of compounds of the form NH<sub>2</sub>C(=X)–YH (X, Y = O or S). This was accomplished by calculating wave functions for the ground states and rotational transition states, subtracting the ground-state charge distribution from that of the transition state, and then visualizing the resulting three-dimensional grid as a contour plot. Charge transfer at the terminal (doubly bonded) oxygen or sulfur was greater for C–N bond rotation than for C–O bond rotation and greater for C–O rotation than for C–S rotation. Transfer to C=S was greater than that to C=O for all rotating groups by roughly a factor of 2, consistent with the behavior that has been observed previously for amides and thioamides. In all cases, the ground state exhibited charge transfer to the terminal carbonyl oxygen or thiocarbonyl sulfur in the  $\pi$  system, partially counteracted by withdrawal in the  $\sigma$  system.

**Acknowledgment.** This investigation was supported by grants from the National Science Foundation (to C.M.H. and to K.B.W.) and the Dreyfus Foundation (to P.R.R.).

**Supporting Information Available:** Extended discussion of molecular geometries as well as tables of absolute energies, zero-point vibrational energies, atomic charges with different basis sets, and geometrical parameters for the molecules considered in this paper (19 pages). This material is contained in libraries on microfiche, immediately follows this article in the microfilm version of the journal, and can be ordered from the ACS; see any current masthead page for ordering information.

JO972180+

(35) Pearson, R. G. *J. Am. Chem. Soc.* **1963**, *85*, 3533.